Exposure to ultraviolet radiation in aquatic ecosystems: estimates of mixing rate in Lake Ontario and the St. Lawrence River

Norman M. Scully, Warwick F. Vincent, and David R.S. Lean

Abstract: Vertical eddy diffusion coefficients (K_z) were determined for the surface waters at several sites in Lake Ontario and along the Upper St. Lawrence River using the water column distribution patterns of hydrogen peroxide. Values of K_z ranged from 0.45×10^{-3} to 23×10^{-3} $m^2 \cdot s^{-1}$ in Lake Ontario and from 0.75×10^{-3} to 2.1×10^{-3} $m^2 \cdot s^{-1}$ along the St. Lawrence River. The residence time for bacterioplankton and phytoplankton in the surface waters was then determined from the K_z values and incorporated into a spectral model to determine the continuous biologically effective exposure to ultraviolet radiation (E^*_{UVR}). The values of E^*_{UVR} for stations where the temperature fine structure profiles indicated near-surface warming (diurnal thermocline formation) were higher (149.1 $J \cdot m^{-2}$) than at stations with isothermal surface waters (3.0 $J \cdot m^{-2}$). Model calculations for two contrasting bays of a lake underscored the dominant role of diurnal thermocline formation in increasing the duration of exposure to continuous damaging ultraviolet radiation exposure. The E^*_{UVR} value for the near-surface bacterioplankton in a humic stained bay was higher (219.2 $J \cdot m^{-2}$) than in a larger bay with lower concentrations of chromophoric dissolved organic matter (47.83 $J \cdot m^{-2}$).

Résumé : Les coefficients de diffusion turbulente verticale (K_z) ont été déterminés pour les eaux de surface de plusieurs sites du lac Ontario et de la partie d'amont du fleuve Saint-Laurent en utilisant les régimes de répartition du peroxyde d'hydrogène de la colonne d'eau. Les valeurs de K_z variaient de $0{,}45 \times 10^{-3}$ à 23×10^{-3} $m^2 \cdot s^{-1}$ dans le lac Ontario et de $0{,}75 \times 10^{-3}$ à $2{,}1 \times 10^{-3}$ $m^2 \cdot s^{-1}$ dans le fleuve Saint-Laurent. Le temps de séjour du bactérioplancton et du phytoplancton dans les eaux de surface a ensuite été déterminé à partir des valeurs de K_z et inclus à un modèle spectral afin de déterminer l'exposition biologiquement efficace continue au rayonnement ultraviolet (E^*_{UVR}). Les valeurs E^*_{UVR} pour les stations où les profils de structure fine de la température indiquaient un réchauffement à proximité de la surface (formation d'une thermocline diurne) étaient plus élevées (149,1 $J \cdot m^{-2}$) que les valeurs aux stations à eaux de surface isothermes (3,0 $J \cdot m^{-2}$). L'application du modèle à deux baies différentes d'un lac a montré le rôle dominant de la formation d'une thermocline diurne pour l'accroissement de la durée d'exposition au rayonnement ultraviolet continue nocif. La valeur E^*_{UVR} pour le bactérioplancton situé à proximité de la surface d'une baie teintée par des matières humiques était plus élevée (219,2 $J \cdot m^{-2}$) que dans une baie à plus faible concentration de matières organiques chromophores dissoutes (47,83 $J \cdot m^{-2}$).

[Traduit par la Rédaction]

Introduction

Intense sunlight causes inhibition of phytoplankton photosynthesis and growth (reviewed by Neale 1987), and many studies have shown that ultraviolet radiation (UVR, 280–400 nm) can negatively impact both bacteria and phytoplankton (Vincent and Roy 1993; Karentz et al. 1994 and references therein). For example, cellular DNA damage increases sharply with decreasing wavelength in laboratory experiments (Setlow 1974); similarly, short-term photoinhibition is a negative function of wavelength (Cullen et al. 1992).

The response of plankton to UVR in the natural environment can be influenced by factors not included in laboratory experiments. During relatively calm periods of intense solar radiation, a near-surface buoyancy gradient or diurnal thermocline can form (Imberger 1985) and restrict the transport of plankton. These conditions can trap phytoplankton near the surface and increase their exposure to UVR and high levels of photosynthetically active radiation (PAR). Conversely, enhanced mixing rates near the surface may reduce the amount of damaging UVR to which an organism is exposed. Milot-Roy and Vincent (1994) found indirect evidence associating UV-induced photoinhibition of phytoplankton with near-surface thermocline formation in a subarctic lake. Furthermore, modeling studies by Neale et al. (1998) demonstrated the critical role of vertical mixing and mixing depth in influencing the photoinhibition of phytoplankton in the water column of Antarctic waters. Bacterioplankton in aquatic systems may also be negatively impacted by UVR. For example, suppressed bacterioplankton activity in the surface waters of the Adriatic Sea was attributed to

Received December 23, 1998. Accepted August 18, 1999. J14948

N.M. Scully and W.F. Vincent. Département de biologie et Centre d'études nordiques, Université Laval, Sainte-Foy, QC G1K 7P4, Canada.
D.R.S. Lean.[1] Department of Biology, University of Ottawa, P.O. Box 450, Station A, Ottawa, ON K1N 6N5, Canada.

[1]Author to whom all correspondence should be addressed. e-mail: dlean@science.uottawa.ca

the more energetic UV-B radiation (280–320 nm) (Herndl et al. 1993). More direct evidence of the effects of surface water mixing on UV-induced damage to aquatic organisms is that DNA dimer formation in bacterioplankton of the Gulf of Mexico was highest when surface water mixing rates were reduced (Jeffrey et al. 1996).

Stratospheric ozone depletion will result in increased UVR, specifically UV-B radiation (280–320 nm). Severe stratospheric ozone depletion has been documented in the Antarctic (Madronich et al. 1991; Schoeberl and Hartmann 1991) and is also occurring in the Arctic (Rex et al. 1997). An overall increase in UV-B radiation for the Northern Hemisphere during winter to early summer has been detected (Kerr and McElroy 1993). Increases in UV-B radiation will further impact the biota of aquatic ecosystems. However, surface water mixing rates may already be a factor controlling the exposure of aquatic organisms to UVR.

UV-absorbing chromophoric dissolved organic matter (CDOM) is an additional control on underwater UVR. Declines in dissolved organic carbon (DOC) through drought-induced acidification can substantially increase the penetration of UV-B radiation in lakes (Yan et al. 1996). Primary productivity in lakes may be positively influenced by CDOM by its effect of screening the phytoplankton from damaging UVR. However, CDOM can also have negative effects by screening PAR, thereby reducing the amount of energy available for primary production. Modeling has demonstrated that CDOM can have this combination of positive and negative effects in the Southern Ocean (Arrigo and Brown 1996). Physical mixing processes in lakes can also be influenced by CDOM. Epilimnetic depths as well as light transparency in small Canadian Shield lakes are correlated with DOC concentration; the depth of the surface mixed layers increased with increasing light transparency and decreasing DOC concentration (Fee et al. 1996). CDOM in freshwater ecosystems may therefore play a pivotal role in controlling UVR exposure to aquatic organisms by limiting UVR penetration and by influencing mixing processes.

In the present study, surface water mixing rates were calculated from depth profiles of hydrogen peroxide (H_2O_2) in Lake Ontario, the Upper St. Lawrence River, and the mouth of the Niagara River and incorporated into a spectral model of UVR based on biological weighting functions for UV damage of DNA. From these model calculations, the roles of surface water mixing rates and diurnal thermocline formation in influencing the biologically effective exposure of bacterioplankton to UVR for the selected study sites were assessed. The role of CDOM in conjunction with mixing rates in influencing the biologically effective exposure of near-surface plankton to UVR was further examined in two contrasting bays of a lake, one more humic stained (higher DOC) than the other.

Materials and methods

Optical and chemical characteristics of the study sites

Experiments were conducted in hydrodynamically contrasting environments in Lake Ontario and the Upper St. Lawrence River (Table 1). Lake Ontario stations 1, 2, and 3 were in midlake regions far from inshore influences whereas station 4 was situated at the mouth of the Niagara River. The river stations (2, 3, 4, and 6) were selected along a transect in the St. Lawrence River (Table 1). UVR and PAR profiles were determined for Lake Ontario stations 1 and 2 and for St. Lawrence station 4 at midday on September 9, 10, and 11, respectively, with a Biospherical PUV-500 profiler. The penetration of both UVR and PAR at the sites was characteristic of large clear systems (Scully and Lean 1994) with relatively low DOC concentrations (3.3–3.5 mg $C \cdot L^{-1}$) (Fig. 1). Vertical downwelling attenuation coefficients were calculated from the profiles of PAR and UVR at 305, 320, 340, and 380 nm (Table 2).

H_2O_2 and temperature profiling

The Lake Ontario and St. Lawrence River stations were sampled for H_2O_2 concentrations at depths of 0.5, 1, 2.5, 5.0, 7.5, 10.0, 12.5, 15, 20, and 25 m from the CSS *Limnos* with 6-L Niskin bottles mounted on a rosette. Temperature measurements were obtained at 0.5-m intervals using a Seabird CTD profiler. Site locations and sampling times for each station are listed in Table 1.

H_2O_2 concentration was determined using the horseradish peroxidase scopoletin method, which involves measuring the enzyme-mediated loss of fluorescence for scopoletin (Cooper et al. 1988; Scully and Vincent 1997). Sample concentrations were calculated from the slope of the change in fluorescence as a function of the H_2O_2 concentration. Calibration curves were obtained through standard additions. Samples were generally analyzed within 15 min of collection.

Brunt–Väisälä frequency

The Brunt–Väisälä frequency (N^2) was calculated every 0.5 m through the water column at each of the sampling sites as a measure of water column stability (Imberger 1985):

$$(1) \qquad N^2 = (-g/\rho_0)(d\rho/dz)$$

where ρ is water density, ρ_0 is the reference water density (10^3 $kg \cdot m^{-3}$), z is depth, and g is acceleration due to gravity (9.8 $m \cdot s^{-2}$).

Eddy diffusivity calculations

Epilimnetic eddy diffusion coefficients (K_z, square metres per second) for diffusion between the photochemically active region and the underlying water within the seasonal mixed zone were estimated at the afternoon sampling sites for which H_2O_2 profiles were recorded. The photochemically active region is defined as the depth stratum where the bulk (99%) of the total water column H_2O_2 is produced (Scully et al. 1998) and its lower limit as the depth of 10% of surface UV-A radiation at 380 nm (Fig. 2). Depth of the photochemically active region (Z_p) is also approximately equivalent to the depth of 1% H_2O_2 production (Scully et al. 1998). The depth of the surface mixed layer (i.e., depth of the diurnal or seasonal thermocline or of the sediments) (Z_m) estimated from temperature profiles at the time of sampling was 2, 16, and 7.5 m for Lake Ontario stations 1, 2, and 3. The estimated surface mixed layer for St. Lawrence River stations 3, 4, 6, and 2 and at the mouth of the Niagara River was 5, 5, 7.5, 17, and 20 m, respectively. The Z_p was estimated to be 3.5 m for all stations (Table 2).

The observed areal H_2O_2 production for the photochemically active region (P_{o_1}, 0–3.5 m) and the underlying stratum (P_{o_2}, 3.5 m to Z_t) (micromoles per square metre per second) was first calculated as $(C_t - C_0)/\Delta t$, where C_t is the areal concentration at sampling time (micromoles per square metre), C_0 is the areal concentration at sunrise (H_2O_2 carryover from the previous day's production) (micromoles per square metre), and Δt is the difference in time (seconds) between sunrise and the sampling time. The subscripts 1 and 2 refer to the photochemically active region and the underlying stratum, respectively. Since early morning profiles were unavailable, a C_0 term for the Lake Ontario and St. Lawrence River sites was estimated with the dark H_2O_2 decay constant of $0.041 \cdot h^{-1}$ for

Table 1. Location and sampling date and time for Lake Ontario and St. Lawrence River stations.

Station	Latitude (N)	Longitude (W)	Sampling date and time (EST)
Lake Ontario			
1	43°25′10″	79°17′57″	9 Sept. 1996, 14:00
2	43°59′59″	76°26′31″	10 Sept. 1996, 09:30
3	43°34′16″	78°16′36″	12 Sept. 1996, 10:00
4	43°15′24″	79°03′30″	12 Sept. 1996, 15:30
St. Lawrence River			
3	44°16′12″	76°02′02″	10 Sept. 1996, 14:00
2	44°38′18″	75°35′59″	11 Sept. 1996, 09:00
6	~44°31′	~75°35′	11 Sept. 1996, 14:00
4	44°23′12″	75°52′10″	11 Sept. 1996, 15:30

Fig. 1. Depth distribution of solar irradiance in Lake Ontario stations (A) 1 and (B) 2 and (C) Upper St. Lawrence River station 4 for 305 (○), 320 (□), 340 (△), and 380 nm UVR (▽) and for PAR (◇).

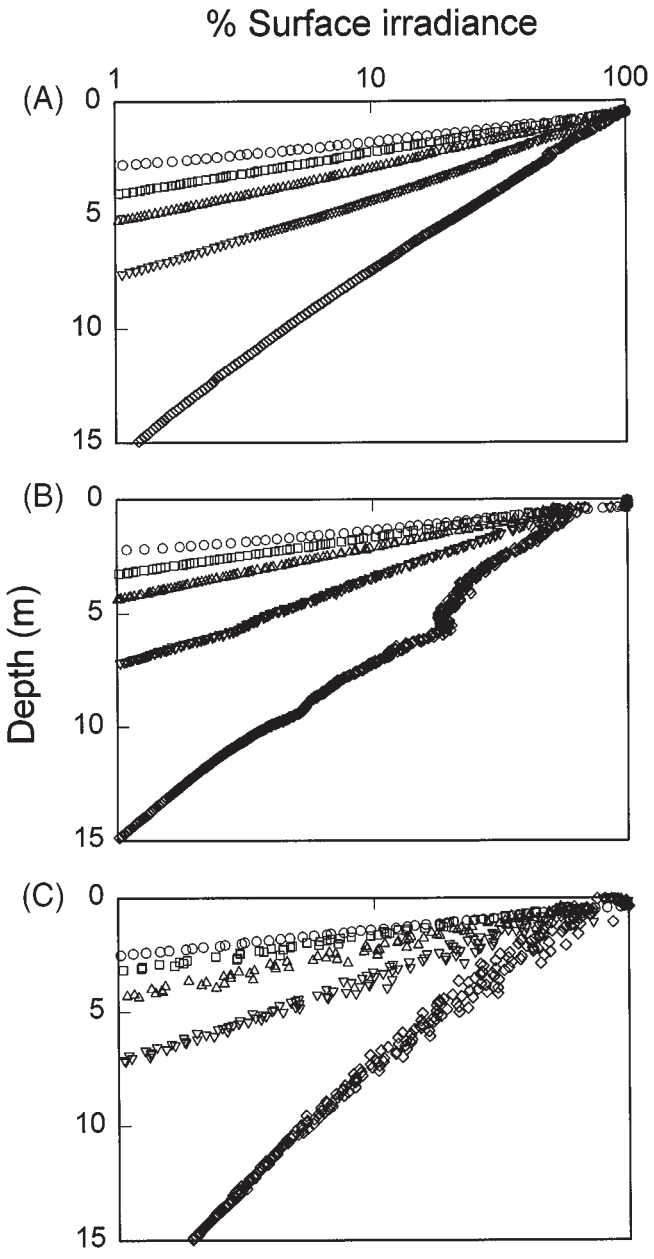

Table 2. DOC and underwater irradiance conditions in Lake Ontario and the St. Lawrence River.

	Lake Ontario		St. Lawrence, station 4
	Station 1	Station 2	
DOC (mg C·L^{-1})	3.5	3.4	3.3
k_λ (305 m) (m^{-1})	1.85	2.18	2.05
k_λ (320 m) (m^{-1})	1.25	1.34	1.43
k_λ (340 m) (m^{-1})	0.94	1.00	1.03
k_λ (380 m) (m^{-1})	0.71	0.62	0.62
k_λ (PAR) (m^{-1})	0.26	0.24	0.24
Z_p (m)	3.2	3.7	3.7
Z_{eu} (m)	17.7	19.2	19.2

Note: k_λ values are the diffuse attenuation coefficients for four UV wavelengths and PAR (400–700 nm), Z_p is the depth of 10% of surface radiation for UV-A (380 nm), and Z_{eu} is the depth of 1% of surface radiation for PAR.

Lake Ontario (Scully et al. 1998), as 68% of C_t at midafternoon. Dark decay constants for H_2O_2 of 0.041·h^{-1} are typical of oligotrophic freshwaters with low DOC concentrations (Scully et al. 1998). The UVR-estimated H_2O_2 areal production (P_e) (H_2O_2 production in the absence of any turbulent diffusion) was then calculated by allocating 99% of the total observed H_2O_2 areal production ($P_{o_1} + P_{o_2}$) to the photochemically active region (P_{e_1}) and 1% to the underlying water column (P_{e_2}). The surface mixed layer areal flux of H_2O_2 associated with turbulent mixing (F, micromoles per square metre per second) was determined by subtracting the observed areal production rate (P_o, micromoles per square metre) from the UVR-estimated areal production rate (P_e, micromoles per square metre):

$$F = P_{e_2} - P_{o_2} \quad (2)$$

The flux of H_2O_2 at depth stratum Z_p was then divided by the difference between the mean concentration in the photochemically active region and that in the waters below ($\Delta[H_2O_2]/Z_t$) Scully et al. (1998). Thus, the calculation of K_z values can be represented by the equation

$$K_z = F/(\Delta[H_2O_2]/Z_t) \quad (3)$$

where K_z is the epilimnetic eddy diffusion coefficient (square metres per second), $\Delta[H_2O_2]$ is the difference between the mean $[H_2O_2]$ in the photochemical zone and the mean $[H_2O_2]$ in the underlying stratum of the epilimnion (micromoles per cubic metre) at C_t, and $Z_t = Z_2 - Z_1$, where Z_1 is the depth (metres) of the center of the photochemically active region and Z_2 is the depth (metres) of the center of the underlying stratum.

Fig. 2. Schematic representation of optical and physical depth limits applied in model calculations. Z_0, beneath the surface; Z_p, limit of the photochemical zone (10% of the UV-A at Z_0); Z_m, depth limit of the diurnal mixed layer; Z_t, depth of the seasonal thermocline; Z_{eu}, depth limit of the euphotic zone.

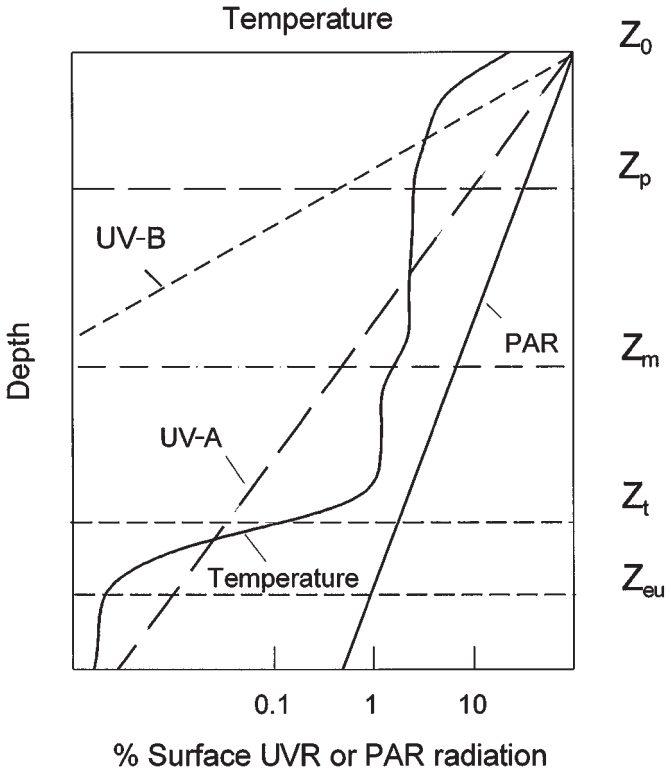

Diffusion time scale

The time scale for a passive particle to diffuse a distance Z in a turbulent flow can be estimated as $Z^2/2K_z$ (Denman and Gargett 1983). This diffuse transport relationship was used to determine the time (t) for a passive particle to diffuse from the surface ($Z = 0$) to the depth of the surface layer (Z_p) (Fig. 2). The above estimate of t was determined assuming an average K_z for the epilimnion (Z_t). A time scale specific to the surface mixed layer was determined with the following equation:

$$t = Z_p^2/2K_z \quad (4)$$

where t is the diffusion time scale (seconds) and Z_p is the depth of the surface layer (metres). By this formulation, t (maximum 6 h) provides an estimate of the residence time of dissolved materials and nonsinking particles in the surface layer.

UVR effective exposure

The primary objective of this study was to determine the impact of surface water mixing rates on the effective exposure for damage by UVR. The biologically effective exposure for UVR was determined for each of the study sites every 2 nm from 280 to 400 nm with biological weighting factor values (ε_λ), diffuse attenuation coefficients (k_λ) (Scully and Lean 1994), UV irradiance measurements (E_λ), and surface water diffusion times (t) (maximum 6 h). This was attained through the following spectral model in which diffusion time was multiplied by the mean irradiance for the upper water column ($E/(k^*Z)(1 - \exp(-k^*Z))$) (Riley 1957) approximated here as $E_\lambda/(k_\lambda Z_p)$ (<0.1% difference between estimates) and by a biological weighting factor (ε_λ) for DNA damage (Setlow 1974):

$$E^*(\lambda) = [(E_\lambda/(k_\lambda Z_p))\varepsilon_\lambda]t. \quad (5)$$

Integrating over the full UVR waveband gives

$$E^*(\lambda) = \frac{t}{Z_p} \int_{\lambda=280\,\mathrm{nm}}^{\lambda=400\,\mathrm{nm}} (E_\lambda \varepsilon_\lambda / k_\lambda)\, \mathrm{d}\lambda \quad (6)$$

where $E^*(\lambda)$ is the biologically effective exposure at wavelength λ, E^* is the biologically effective exposure integrated over the full UVR waveband. (joules per square metre), $E_\lambda/(k_\lambda Z_p)$ is the average surface layer exposure, E_λ is the exposure at a specific wavelength (joules per square metre per nanometre), k_λ is the diffuse attenuation coefficient (per metre) (Scully and Lean 1994), and ε_λ is the biological weighting factor (Setlow 1974). The biological weighting factor values for DNA damage were obtained from Setlow (1974) and calculated every 2 nm from 280 to 400 nm, as in Milot-Roy and Vincent (1994). Biological weighting factor values were normalized to 1 at 300 nm. Spectral solar irradiance (280–800 nm every 2 nm) (E_λ) was measured over Lake Erie on a cloudless day, 13 July 1994, from 06:00 to 21:00 every 15–30 min with an OL 752 Optronics double monochromator scanning spectroradiometer (Scully et al. 1997). Measured spectra were then integrated over the period 12:00–18:00 to obtain a midday UVR exposure value. Because the PUV instrument does not have fine wavelength resolution in the UV-B region, we applied to our model calculation the attenuation coefficients (2 nm from 280 to 400 nm) for Lake Ontario from Scully and Lean (1994).

There was very little variability in UVR penetration at the Lake Ontario and St. Lawrence River stations. To evaluate the effect of UVR attenuation by CDOM on the effective exposure, modeled $E^*(\lambda)$ and E^* values were also determined for two optically different bays (one humic stained and the other relatively clear) in a small lake in central Ontario, Canada (Jacks Lake, 43°70′N, 78°02′W). Diffusion time scale values for bacteria and phytoplankton were calculated from Scully et al. (1998), where H_2O_2-derived K_z values were determined concurrently for Brookes Bay (humic stained) and Sharpes Bay (relatively clear) over 3 consecutive days. Model parameter values (K_z, t, Z_p, Z_t, and Z_m) applied in calculating $E^*(\lambda)$ and E^* for both sites are listed in Table 3.

Results

Temperature, N^2, and H_2O_2 profiles

Profiles of temperature and N^2 values at Lake Ontario station 1 (14:00) indicate the formation of a near-surface thermocline (<2 m) (Fig. 3A). Temperature and N^2 profiles at Lake Ontario stations 3, 2, and 4 (Figs. 3B, 3C, and 3D) indicate generally isothermal surface water column conditions. A temperature gradient occurred at 7.5 m at station 3 (Fig. 3B). H_2O_2 was generally evenly distributed at the surface (0–7.5 m) at all Lake Ontario stations with the exception of station 1 where there was a surface concentration gradient at a depth of about 2 m.

Weak surface thermoclines were also present at St. Lawrence River stations 3 and 6 (Figs. 4A and 4B), which contrasted with the isothermal water column of station 2 (Fig. 4D). Isothermal conditions (as measured at a scale of 0.5 m) were also present at station 4 but only for <5 m (Fig. 4C). Peaks in N^2 values ($4.0 \times 10^{-4} \cdot s^{-2}$) were present at the surface of stations 3, 6, and 4. There were no N^2 peaks present at station 2. H_2O_2 concentration profiles for the St. Lawrence River stations were uniform in distribution and followed patterns similar to temperature and N^2 values and are consistent with a statistically significant correlation be-

Table 3. Limnological characteristics of Sharpes Bay and Brookes Bay (Jacks Lake, central Ontario) and mixing parameters derived from H_2O_2 profiling (Scully et al. 1998).

	Sharpes Bay	Brookes Bay
Area (km^2)	5.1	0.85
Fetch (km)	3.0	1.5
DOC (mg $C \cdot L^{-1}$)	5.6	7.6
Z_p (m)	1.0	0.5
Z_{eu} (m)	4.26	4.04
Z_t (m)	5.0	3.0
K_z (10^{-5} $m^2 \cdot s^{-1}$)		
Day 1	11 (±0.35)	0.35 (±0.1)
Day 3	36 (±1.2)	2.1 (±0.1)
t (h), Z_m (m)		
Day 1	1.3, 2.0	9.9, 0.5
Day 3	0.4, 5.0	1.6, 3.0

Note: Z_p is the depth of 10% of surface radiation for UV-A (380 nm), Z_{eu} is the depth of 1% of surface radiation for PAR, Z_t is the depth of the epiliminion, K_z is the surface water vertical eddy diffusivity, t is the diffusion time, and Z_m is the mixed layer depth. Standard deviations for K_z values (given in parentheses) were calculated by propagation of errors.

tween H_2O_2 distribution patterns and N^2 values determined in an earlier study by Scully and Vincent (1997). H_2O_2 was generally evenly distributed through the water column at stations 4 and 2 (Figs. 4C and 4D) but with H_2O_2 concentration gradients at the surface of stations 3 and 6 (Figs. 4A and 4B).

Eddy diffusivity and diffusion time scale

Calculated eddy diffusivity and diffusion time at stations with a near-surface thermocline were lower than at stations with an isothermal water column. The estimated K_z value at Lake Ontario station 1 was 0.45×10^{-3} $m^2 \cdot s^{-1}$ whereas at the mouth of the Niagara River (Lake Ontario station 4), the value was 23×10^{-3} $m^2 \cdot s^{-1}$ (Table 4). Along the St. Lawrence River, K_z values ranged from 0.8×10^{-3} $m^2 \cdot s^{-1}$ for station 3 to 2.1×10^{-3} $m^2 \cdot s^{-1}$ for station 4. Surface water diffusion time values for Lake Ontario stations 4 and 1 were 0.07 and 3.7 h, respectively, whereas values at stations along the St. Lawrence River stations ranged from 0.7 (station 4) to 2.2 h (station 3) (Table 4).

Effective exposure

The effective exposure (E^*) in the wavelength range 280–400 nm was influenced by diurnal thermocline formation. Increased diffusion time and surface irradiance at the surface waters of Lake Ontario station 1 resulted in $E^*(\lambda)$ values that were greater than at the mouth of the Niagara River (Fig. 5A). Similarly, the St. Lawrence River station 3 values were higher than the St. Lawrence River station 4 values (Fig. 5B).

The relative response in modeled values in Sharpes Bay and Brookes Bay was also dependent on the surface water diffusion time and irradiance. Day 1 of the experiment was calm relative to the more windy day 3, and subsequently, there was the formation of a near-surface diurnal thermocline in Brookes Bay and Sharpes Bay between 14:00 and 17:00 (Scully et al. 1998). The formation of a near-surface thermocline on day 1 resulted in a relatively high surface layer diffusion time/irradiance and hence higher modeled values than on day 3 (Fig. 6).

As expected, the $E^*(\lambda)$ values for DNA damage were limited to the UV-B region (280–320 nm), with the highest values at approximately 305 nm. Differences between the lakes are further underscored by comparing integrated E^*. Values for UV-B effective exposure of 47.8 and 14.6 $J \cdot m^{-2}$ were calculated for Sharpes Bay obtained on days 1 and 3. In Brookes Bay on day 1, the E^* value was more than four times higher (219.2 and 60.4 $J \cdot m^{-2}$, respectively). The $E^*(\lambda)$ values for the region below the surface layer but within the seasonal mixed layer zone were also calculated (t = 6 h) and were always <1% of the surface layer values.

Discussion

This study demonstrates the prominent role of diurnal thermocline formation in controlling the exposure of planktonic organisms to damaging levels of UV-B radiation. The $E^*(\lambda)$ values for the two Lake Ontario sites were representative of the general hydrodynamic conditions of the water column of the two sites. The effective exposure to UV-B, during a transit of the surface layer, was higher at the mid-lake station, where there was a near-surface buoyancy gradient, than at the station at the mouth of the Niagara River with an isothermal, and likely well-mixed, water column. The presence of a weak surface thermocline was also likely responsible for the greater biologically effective exposure at stations 3, 4, and 6. The study is consistent with observations that diurnal thermocline formation was associated with UV-induced damage (Milot-Roy and Vincent 1994) where photosynthesis of different size-classes of phytoplankton was measured under various UVR regimes at several sites in a morphometrically diverse subarctic lake. The mixing and stratification processes at the sites were determined through fine-scale temperature measurements. The formation of steep near-surface temperature gradients was detected at several stations and was proposed as a significant factor in prolonging the residence time of phytoplankton near the surface and thus increasing their exposure to damaging UVR. Similar effects of PAR as well as UVR were observed at Lake Titicaca, South America (Vincent et al. 1984). Bacterioplankton in aquatic ecosystems may be similarly affected by surface water mixing rates. Jeffrey et al. (1996) found the accumulation of UV-induced DNA dimers in the surface water of the Gulf of Mexico to be significantly higher under calm conditions than under apparently turbulent surface waters.

Although in the present study, there were no in situ measures of phytoplankton photoinhibition or UV-induced DNA damage, the model calculations of $E^*(\lambda)$ provide a more quantitative estimate of the role of surface water mixing rates in controlling UV-B exposure of aquatic organisms than has been previously available. It should also be noted that the estimates of K_z, and hence t values, determined for the present study were averages for the epilimnion. Since the epilimnia of lakes are composed of many layers with variable mixing rates and overturn lengths (Imberger and Spigel

Fig 3. Temperature (solid line) and H_2O_2 (solid line with circles) and N^2 (dotted line) profiles for Lake Ontario stations (A) 1, (B) 3, (C) 2, and (D) 4.

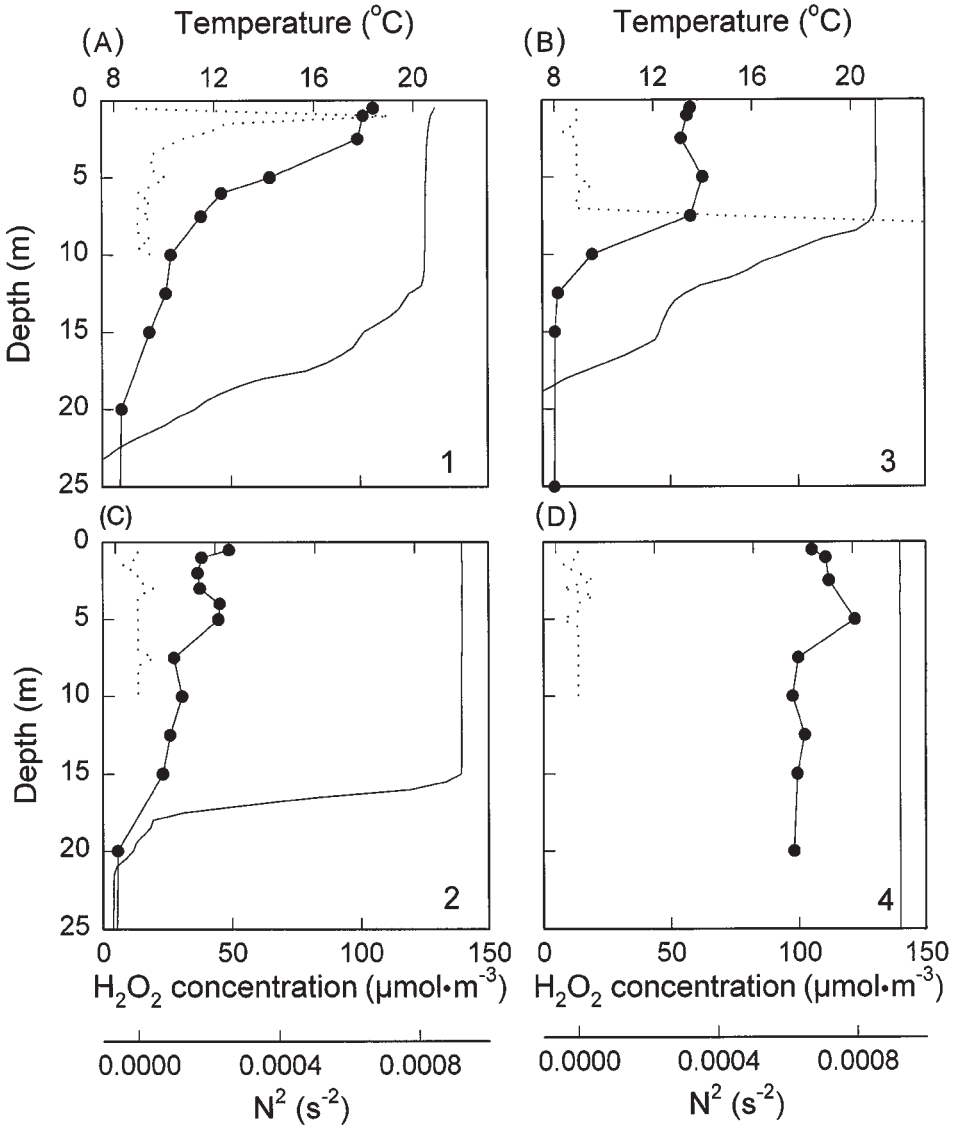

1987), the $E^*(\lambda)$ values presented here are representative of hydrodynamic processes integrated over time and depth. Consequently, the application of average epiliminetic K_z values may underestimate the effective exposure for the surface layer. Furthermore, these values are specific to the surface layer of the study sites. Phytoplankton and bacteria within the euphotic zone but beneath the diurnal mixed layer would be more effectively screened from UV-B (i.e., in the depth region of 4–18 m in the St. Lawrence River and Lake Ontario and 2–4 m in Sharpes Bay). These regions of the water column are therefore subjected to a generally more favourable light climate than those within the diurnal mixed layer (low UVR and moderate PAR levels). Additionally, DNA shielding may reduce the impact of UV-B-induced DNA damage to bacteria.

Under calm clear conditions, near-surface temperature gradients can form and persist for several hours during the day. During these periods of near-surface warming, solar radiation (UVR and PAR) is generally high. The link between diurnal thermocline formation and DNA damage to phytoplankton and bacteria is therefore particularly relevant vis-à-vis the impact of UV-B in the natural environment. It should also be noted that although damage integrated over the water column is similar under a stratified water column and under a well-mixed water column, repair processes under both scenarios are likely to occur at different time scales and rates. The intense continuous midday exposure encountered by microbial communities within a diurnal layer will result in an altogether different damage repair dynamic than in those receiving moderate and (or) intermittent UV-B exposure within a mixed water column. The E^* provides a measure of the continuous exposure of cells to damaging UV irradiance and also to potentially toxic levels of H_2O_2 and other reactive oxygen species (Xenopoulous and Bird 1997). Intermittent exposure to UV and transport out of the region 0 m to Z_p will allow cells to recover to an extent that depends on the time scale of recovery and the residence time in the region Z_p to Z_m. In some systems, the exposure to

Fig 4. Temperature (solid line) and H_2O_2 (solid line with circles) and N^2 (dotted line) profiles for Upper St. Lawrence River stations (A) 3, (B) 6, (C) 4, and (D) 2.

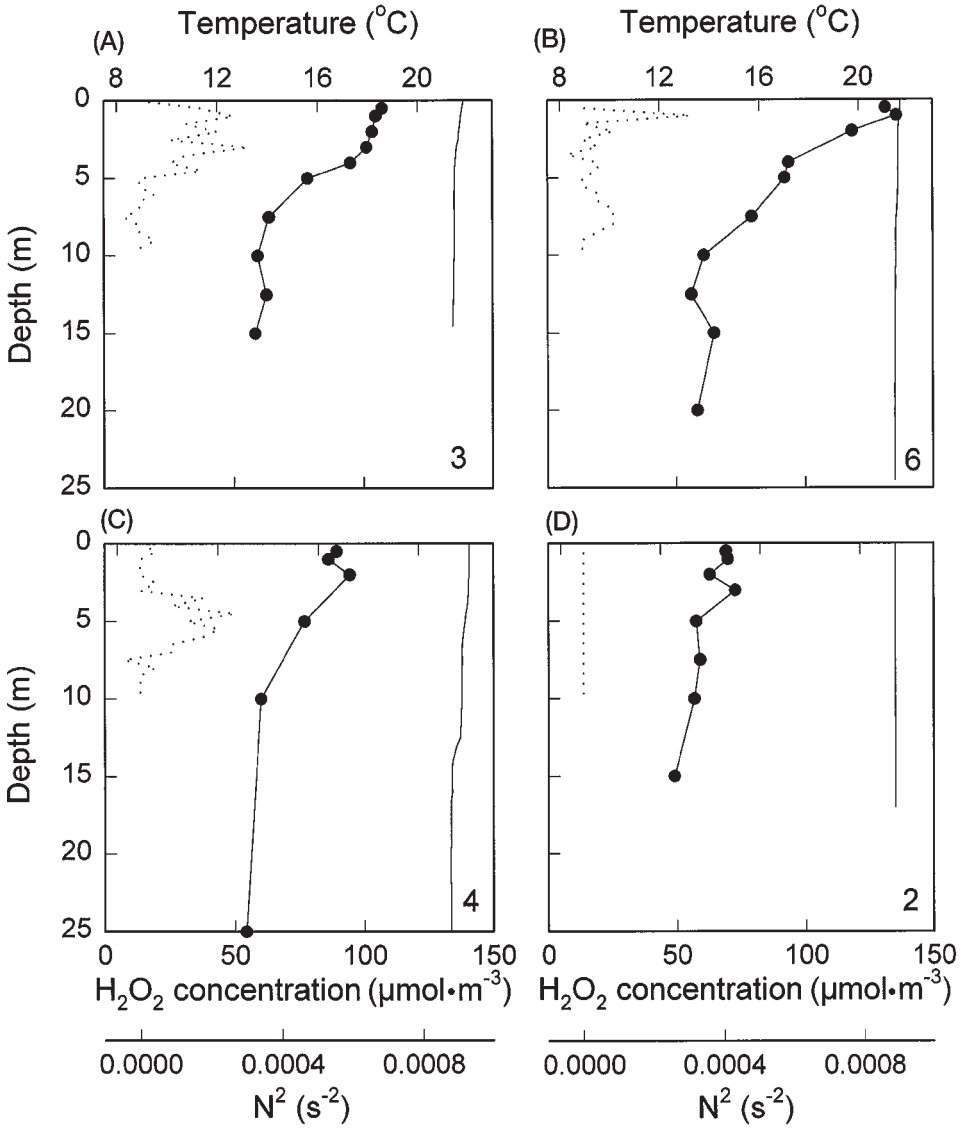

Table 4. Surface water vertical eddy diffusivities (K_z), diffusion times (t), mixed layer depth (Z_m), and epilimnion or seasonal mixed layer depth (Z_t) for Lake Ontario and St. Lawrence River stations.

Station	K_z (10^{-3} $m^2 \cdot s^{-1}$)	t (h)	Z_m (m)	Z_t (m)
Lake Ontario				
1	0.45 (±0.08)	3.7	2.0	15.0
4	23.0 (±2.7)	0.07	20.0	20.0
St. Lawrence River				
3	0.8 (±0.1)	2.2	5.0	15.0
4	2.1 (±0.25)	0.7	5.0	15.0
6	1.9 (±0.2)	0.9	7.5	20.0

Note: Standard deviations (given in parentheses) were calculated by propagation of errors.

damaging UV may be so brief and (or) the recovery from this intermittent exposure so rapid that any discernable effects of damage may be eliminated (e.g., Gulf of Mexico, Jeffrey et al. 1996). In other systems, however, the rate of recovery is so slow that cells may be entrained back into the region 0 m to Z_p before recovery takes place, and the damaging effects of UV exposure will be compounded. Such effects are likely under low temperatures (Roos and Vincent 1998) and may operate in the Southern Ocean (Neale et al. 1998). For the latter systems, it may be more appropriate to scale E^* to Z_m rather than to Z_p, i.e.,

$$E^* = \int_{\lambda=280\text{nm}}^{\lambda=400\text{nm}} (E_\lambda \varepsilon_\lambda / k_\lambda Z_m)\, d\lambda .$$

Prolonged near-surface exposure to UV-B may be particularly common for planktonic organisms in small (<500 ha) lakes with high CDOM levels where, because of limited wind fetches and near-surface absorption of solar radiation, steep near-surface temperature gradients are formed. The formation of these near-surface temperature gradients in aquatic ecosystems such as Brookes Bay is relatively commonplace (Imberger 1985). The modeled E^* values in the

Fig 5. Biologically effective exposure for DNA damage from 290 to 360 nm for (A) Lake Ontario stations 1 and 4 (in descending order) and (B) St. Lawrence stations 4, 6, and 3 (in descending order). The dotted line represents the biologically effective exposure values below the diurnal mixed layer.

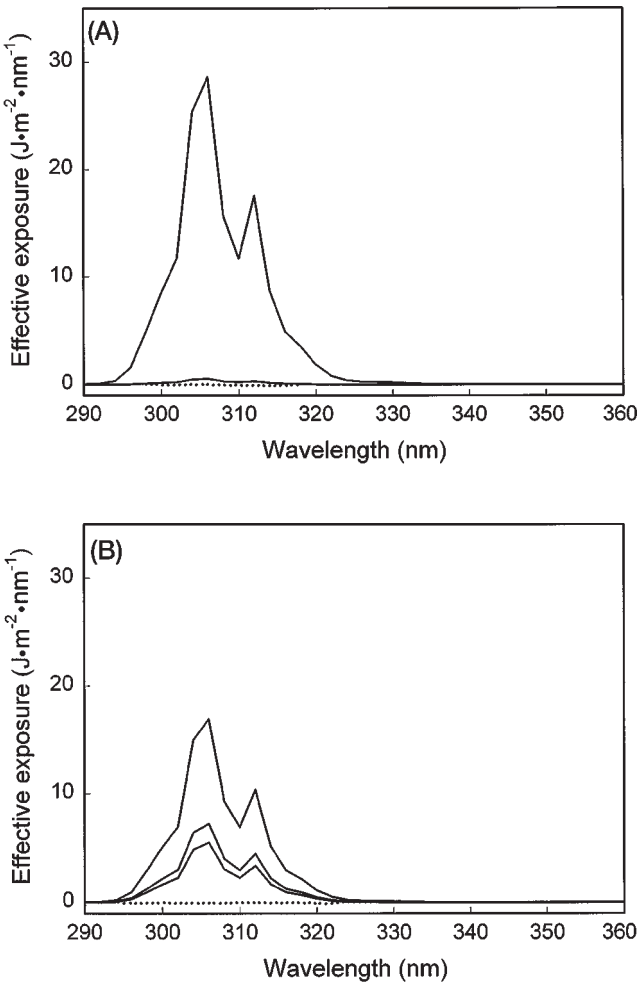

Fig 6. Biologically effective exposure for DNA damage from 290 to 360 nm for surface waters of (A) Brookes Bay and (B) Sharpes Bay on days 1 and 3 (in descending order). The dotted line represents the biologically effective exposure values below the diurnal mixed layer.

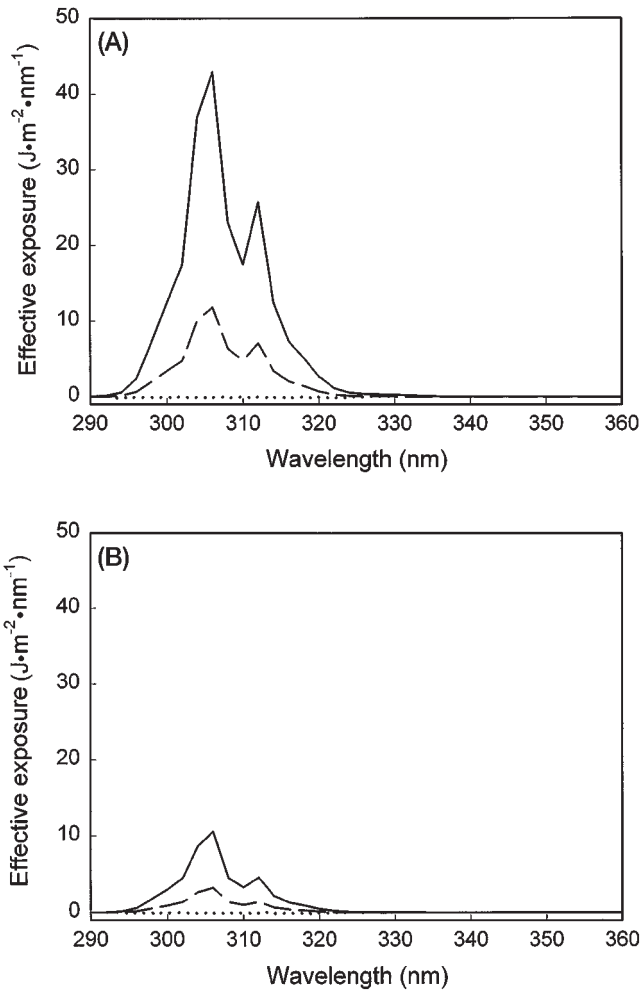

humic-stained Brookes Bay were higher than in Sharpes Bay. Although the smaller size of Brookes Bay was likely a more significant contributing factor to lower surface water mixing rates, the greater light-absorbing properties of this bay relative to Sharpes Bay may also have contributed to the decreased mixing rates. A correlative relationship exists between water transparency and epilimnetic depth for small Canadian shield lakes (Fee et al. 1996). Similarly, diurnal thermocline formation and persistence in small lakes may also be influenced by CDOM-mediated water transparency.

DOC concentrations in lakes may be reduced through processes such as acidification and climate change, with resultant increases in the penetration of UVR in lakes (Schindler et al. 1996; Yan et al. 1996). The results of our study, however, imply that increased light penetration in small lakes may actually decrease the near-surface exposure of bacterioplankton to UV-B through increased susceptibility to mixing and thus decreased surface water residence time. With increased light penetration, there may be a concomitant increase in phytoplankton photosynthesis, since more PAR would be available in the water column. The opposing roles of CDOM in both enhancing primary production (by limiting UVR) and reducing primary production (by limiting PAR) were noted earlier through model calculations by Arrigo and Brown (1996). However, their study did not address the role of surface water mixing rates in influencing UV-B exposure of phytoplankton. The exposure model developed in the present study underscores the critical importance of near-surface residence times and provides an approach towards estimating the biological effects of changing UV-B (via ozone depletion or climatic effects on CDOM) in the surface strata of dynamic mixed layer environments.

Acknowledgements

We thank the crew of the CSS *Limnos* for their assistance during the sampling cruise on Lake Ontario and the St. Lawrence River. We also thank John Gibson, Ladd Johnson, and Peter Leavitt for helpful comments. Patrick Neale and an anonymous referee provided invaluable reviews. Financial support was provided by research funds from the Natural

Sciences and Engineering Research Council of Canada, Fonds pour la Formation de Chercheurs et l'Aide à la Recherche (Québec, Canada), and a Canada–U.S. Environment Canada Fulbright scholarship to N.M.S.

References

Arrigo, K.R., and Brown, C.W. 1996. Impact of chromophoric dissolved organic matter on UV inhibition of primary productivity in the sea. Mar. Ecol. Prog. Ser. **140**: 207–216.

Cooper, W.J., Zika, R.G., Petasne, R.G., and Plane, J.M.C. 1988. Photochemical formation of H_2O_2 in natural waters exposed to sunlight. Environ. Sci. Technol. **22**: 1156–1160.

Cullen, J.J., Neale, P.J., and Lesser, M.P. 1992. Biological weighting function for the inhibition of phytoplankton photosynthesis by ultraviolet radiation. Science (Washington, D.C.), **258**: 646–650.

Denman, K.L., and Gargett, A.E. 1983. Time and space scales of vertical mixing and advection of phytoplankton in the upper ocean. Limnol. Oceanogr. **28**: 801–815.

Fee, E.J., Hecky, R.E., Kasian, S.E., and Cruikshank, D.R. 1996. Effects of lake size, water clarity and climatic variability on mixing depths in Canadian Shield lakes. Limnol. Oceanogr. **41**: 912–920.

Herndl, G.J., Muller-Niklas, G., and Frick, J. 1993. Major role of ultraviolet-B in controlling bacterioplankton growth in the surface layer of the ocean. Nature (Lond.), **361**: 717–719.

Imberger, J. 1985. The diurnal mixed layer. Limnol. Oceanogr. **30**: 737–770.

Imberger, J., and Spigel, R.H. 1987. Circulation and mixing in Lake Rotongaio and Lake Okaro under conditions of light to moderate winds: preliminary results. N.Z. J. Mar. Freshwater Res. **21**: 361–377.

Jeffrey, W.H., Aas, P., Lyons, M.M., Coffin, R.B., Pledger, R.J., and Mitchell, D.L. 1996. Ambient solar radiation-induced photodamage in marine bacterioplankton. Photochem. Photobiol. **64**: 419–427.

Karentz, D., Bothwell, M.L., Coffin, R.B., Hanson, A., Herndl, G.J., Kilham, S.S., Lesser, M.P., Lindell, M., Moeller, R.E., Morris, D.P., Neale, P.J., Sanders, R.W., Weiler, C.S., and Wetzel, R.G. 1994. Impact of UV-B radiation on pelagic freshwater ecosystems: report of working group on bacteria and phytoplankton. Arch. Hydrobiol. Beih. Ergebn. Limnol. **43**: 31–69.

Kerr, J.B., and McElroy, C.T. 1993. Evidence for large upward trends of ultraviolet-B radiation linked to ozone depletion. Science (Washington, D.C.), **262**: 1032–1034.

Madronich, S., Bjorn, L.O., Ilyas, M., and Caldwell, M.M. 1991. Changes in biologically active ultraviolet radiation reaching the earth's surface. *In* Environmental effects of ozone depletion: 1991 update. Chap. 1. United Nations Environment Program Publication, New York. pp. 1–14.

Milot-Roy, V., and Vincent, W. 1994. UV radiation effects on photosynthesis: the importance of near-surface thermoclines in a subarctic lake. Arch. Hydrobiol. Beih. Ergebn. Limnol. **43**: 171–184.

Neale, P.J. 1987. Algal photoinhibition and photosynthesis in the aquatic environment. *In* Photoinhibition. *Edited by* D.J. Kyle, C.B. Osmond, and C.J. Arntzen. Elsevier, Amsterdam, The Netherlands. pp. 39–66.

Neale, P.J., Davis, R.F., and Cullen, J.J. 1998. Interactive effects of ozone depletion and vertical mixing on photosynthesis of Antarctic phytoplankton. Nature (Lond.), **392**: 585–589.

Rex, M., Harris, N.R.P., von der Gathen, P., Lehmann, R., Braathen, G.O., Reimer, E., Beck, A., Chipperfield, M.P., Alfier, R., Allaart, M., O'Conner, F., Dier, H., Dorokhov, V., Fast, H., Gil, M., Kyro, E., Litynska, Z., Mikkelsen, I.S., Molyneux, M.G., Nakane, H., Notholt, J., Rummukainen, M., Viatte, P., and Wenger, J. 1997. Prolonged stratospheric ozone loss in the 1995–96 Arctic winter. Nature (Lond.), **389**: 835–837.

Riley, G.A. 1957. Phytoplankton of the North Central Sargasso Sea. Limnol. Oceanogr. **2**: 252–270.

Roos, J., and Vincent, W.F. 1998. Temperature dependence of UV radiation effects on Antarctic cyanobacteria. J. Phycol. **34**: 78–85.

Schindler, D.W., Curtis, P.J., Parker, B.R., and Stainton, M.P. 1996. Consequences of climate warming and lake acidification for UV-B penetration in North American boreal lakes. Nature (Lond.), **379**: 705–708.

Schoeberl, M.R., and Hartmann, D.L. 1991. The dynamics of the stratospheric polar vortex and its relation to springtime ozone depletions. Science (Washington, D.C.), **251**: 46–52.

Scully, N.M., and Lean, D.R.S. 1994. The attenuation of ultraviolet radiation in temperate lakes. Arch. Hydrobiol. Beih. Ergebn. Limnol. **43**: 135–144.

Scully, N.M., and Vincent, W.F. 1997. Hydrogen peroxide: a natural tracer of stratification and mixing processes in subarctic lakes. Arch. Hydrobiol. **139**: 1–15.

Scully, N.M., Vincent, W.F., Lean, D.R.S., and Cooper, W.J. 1997. Implications of ozone depletion for surface-water photochemistry: sensitivity of clear lakes. Aquat. Sci. **59**: 1–15.

Scully, N.M., Vincent, W.F., Lean, D.R.S., and MacIntyre, S. 1998. Hydrogen peroxide as a natural tracer of mixing. Aquat. Sci. **60**: 169–186.

Setlow, R.B. 1974. The wavelengths in sunlight effective in producing skin cancer: a theoretical analysis. Proc. Nat. Acad. Sci. U.S.A. **71**: 3363–3366.

Vincent, W.F., and Roy, S. 1993. Solar ultraviolet radiation and aquatic primary production: damage, protection, and recovery. Environ. Rev. **1**: 1–12.

Vincent, W.F., Neale, P.J., and Richerson, P.J. 1984. Photoinhibition: algal responses to bright light during diel stratification and mixing in a tropical alpine lake. J. Phycol. **20**: 201–211.

Yan, N.D., Keller, W., Scully, N.M., Lean, D.R.S., and Dillon, P.J. 1996. Increased UV-B penetration in a lake owing to drought-induced acidification. Nature (Lond.), **381**: 141–143.

Xenopoulous, A., and Bird, D.F. 1997. Effect of acute exposure to hydrogen peroxide on the production of phytoplankton and bacterioplankton in a mesohumic lake. Photochem. Photobiol. **66**: 471–478.